III Всероссийская научная конференция с международным участием «Наука, технологии, общество: Экологический инжиниринг в интересах устойчивого развития территорий» (НТО-III) при поддержке Краевого фонда науки

6 (2022)

УДК 658.512.011 DOI 10.47813/nto.3.2022.6.109-124 EDN IQDKDO

Контроль погрешностей идентификации и фильтрации изображений микрообъектов

И.И. Жуманов, Р.А. Сафаров*, О.И. Джуманов

Самаркандский государственный университет, Университетский бульвар, 15, Самарканд, 140104, Узбекистан

*E-mail: rustammix.rs@gmail.com

Аннотация Исследованы и разработаны научно-методологические основы оптимальной идентификации микрообъектов с применением традиционных и гауссовой фильтрации, медианного фильтра, фильтров, основанных на быстром преобразовании Фурье (БПФ), вейвлет – преобразований (ВП), сдвиг – преобразований, механизмов, использующих геометрические, специфические особенности статистических, динамических свойств информации в изображениях. Предложены механизмы оптимизации идентификации микрообъектов, обладающих преимуществами при снижении сложности, трудоемкости анализа структуры и обработки информации, выявлении и сегментации контура изображения, использовании динамики роста, визуального разграничения, извлечении внутренних особенностей и свойств, аппроксимации, сглаживании, интерпретации объектов. Исследован и реализован механизм, который выполняет следующие функции: выравнивает срезы гистологии; находит контура объектов, набор уровней, пороги, сочетает сегментации, проводит регистрации, формирует граф поиска, выполняет аппроксимации на основе вейвлет, сдвиговых и других преобразований, определяет параметры, производит цветовое кодирование и цветовую визуализацию микрообъектов. Протестированы реализации алгоритмов и программных модулей программного комплекса идентификации, распознавания и классификации микрообъектов, в частности клеточных элементов воспалительного ряда (фибробластов, фиброцитов) болезни легких. Оценивались признаки хронического воспаления – наличие гигантских клеток. Разработан программный комплекс визуализации, распознавания, классификации изображений пыльцевых зерен, реализации которого протестированы с учетом условий априорной недостаточности, параметрической неопределенности и нестационарности процессов.

Ключевые слова: изображение, пыльцевые зерна, идентификация, обработка информации, погрешность, механизмы контроля.

Error Control of Identification and Filtering of Micro-Object Images

I.I. Jumanov, R.A. Safarov*, O.I. Djumanov

Samarkand state university, University boulevard, 15, 140104 Samarkand, Uzbekistan

*E-mail: rustammix.rs@gmail.com

Abstract Researched and developed scientifically and methodologically foundations for optimal identification of micro-objects using traditional and Gaussian filtering, median filter, filters based on fast Fourier transform, wavelet transforms, shift transforms, mechanisms using geometric, specific features, statistical, dynamic properties of image information. Mechanisms for optimizing the identification of micro-objects are proposed that have advantages in reducing the complexity and laboriousness of analyzing the structure and processing information, identifying and segmentation of the image contour, using the dynamics of growth, visual differentiation, extracting internal features and properties, approximation, smoothing, and interpretation of objects. A mechanism has been investigated and implemented that performs the following functions: aligns histology slices; finds contours of objects, a set of levels, thresholds, combines segmentation, conducts registrations, forms a search graph, performs approximations based on a wavelet, shear, and other transformations, determines parameters, performs color coding and color visualization of micro-objects. The implementations of algorithms and software modules of the software complex for identification, recognition and classification of micro-objects, in particular, cellular elements of the inflammatory series (fibroblasts, fibrocytes) of lung disease, have been tested. The signs of chronic inflammation were assessed - the presence of giant cells. A software package for visualization, recognition, classification of images of pollen grains has been developed, the implementations of which have been tested taking into account the conditions of a priori insufficiency, parametric uncertainty and nonstationarity of processes.

Keywords: image, pollen grains, identification, information processing, error, control mechanisms.

1. Intoduction

Of great importance is the study of methods for digital processing of images of micro-objects, in particular, the development of practical applications related to the recognition of pollen grains, unicellular microorganisms, pictures of useful minerals in the rock mass, which are in great demand in palynology, medicine, ecology, biology, mining technology and others [1, 2, 4, 6].

Recognition and classification of micro-objects, in turn, are associated with the optimization of image identification based on the use of mechanisms that eliminate the noise component - interference, "debris" in the composition of pollen, contrast defects, brightness, which are implemented using numerical modeling, geometric, morphological, texture analysis, as well as using mechanisms for extracting statistical, dynamic and specific characteristics of images [7, 8, 9, 10, 11].

This study is devoted to the development of methods and technology for the identification of micro-objects using the fast Fourier transform (FFT), wavelet transforms (WT), shear mechanisms based on the use of Gaussian transformations with mechanisms for using geometric, specific features, statistical, dynamic properties of information about images, and also mechanisms using structural connections, functions, factors of influence on the process of recognition of micro-objects [14, 15-20].

The proposed technology for identifying micro-objects has advantages in reducing the complexity and laboriousness of structure analysis and image processing, identifying and segmentation of the contour, using growth dynamics, visual differentiation, extracting internal features and properties, increasing the accuracy of approximation, smoothing, and image interpretation.

2. Main part

2.1. Constructive approaches, principles and methods for optimizing the identification of images of micro-objects

When solving problems of identification, recognition and classification of micro-objects, microscopic digital photography, scanning electron microscopy are used, in the images of which defects appear caused by the presence of noise, "debris", uneven contrast, low brightness leading to a decrease in the accuracy of image identification.

To reduce the systematic identification error, the following trivial mechanisms are used: control based on the extraction of statistical parameters - mathematical expectation, variance, correlation function, distribution laws; noise reduction; brightness settings; alignment and contrast correction. The proposed mechanisms include dynamic models, algorithms, rules for extracting and using the properties of information and images of micro-objects when optimizing the values of the determining parameters. In figure 1 shows a graphical principle of control of the systematic error in image identification by function $y = f(t)$ by isolating real random and constant components.

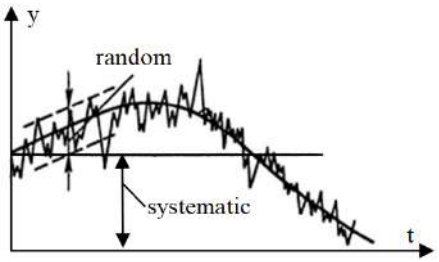

Figure 1. Error Control Principle.

Mechanisms with multiple measurements, obtaining arithmetic mean values of error, variance, and distribution laws are also used. A digital image presented in a coordinate space is viewed by a three-component and two-dimensional signal. Each $L \times M$ image element represents a vector

$$C(l,m) = \left[R(l,m), G(l,m), B(l,m)\right],$$

where l - line number; m - column number $l \in [0, L-1]$, $m \in [0, M-1]$; $R(l,m)$, $G(l,m)$, $B(l,m)$ - element components with coordinates (l,m).

In the study, the following generalizations of the statistical parameters of the image information are indicated:

$R(l,m)$ - mathematical expectation, variance, correlation function;

$G(l,m)$ - law of distribution, noise reduction, brightness;

$B(l,m)$ - image contrast alignment and correction.

The function of the distance between two vectors numbered i and j is introduced, which is given in the form $d_{ij} = \left\| C_i - C_j \right\|_\gamma = \left(\sum_{n=1}^{3} \left| C_i^n - C_j^n \right|^\gamma \right)^{1/\gamma}$, n - vector component number; γ

- euclidean distance characteristic $d_{ij} = \|C_i - C_j\| = \sqrt{(R_i - R_j)^2 + (G_i - G_j)^2 + (B_i - B_j)^2}$. The input vector in the sliding filtering window is given by $W = \{C_0, C_1, ..., C_{p-1}\}$, $C_i = (R_i, G_i, B_i), i \in [0, p-1]$.

Mechanisms that perform the following functions have been investigated and implemented: alignment of histology slices; finding the contour of selected local areas of objects, forming a set of points of image texture levels, determining thresholds, combining segmentation procedures, forming a search graph, performing approximation, wavelet-shift and other transformations, producing color coding and visualizations, determining model parameters. The features of the mechanisms are the use of geometric, statistical, specific, dynamic characteristics of images and properties of information. Due to the application of this approach to image processing, mechanisms have advantages in reducing the complexity, laboriousness of structure analysis and information processing, image segmentation, the use of growth dynamics, visual differentiation, extraction of internal features and properties, and interpretation of objects.

An image identification mechanism with a median filter is proposed, which suppresses the high frequencies of the systematic error in image identification, causing blurring of edges and textures. The structure of the systematic identification error includes errors due to errors in input, transmission, processing of information; errors associated with the effects of noise, blur and other nature of defects on the image. We have obtained analytical expressions for estimates of the systematic identification error for various models, in particular, biquadratic, polynomial, statistical, regression dynamic models. The obtained results of the study involve mathematical expressions for estimates of error probabilities, simplified estimates of mathematical expectation, variance, autocorrelation functions, and other parameters. The results obtained are used to assess the qualitative characteristics of the recognition and classification of micro-objects. In the filtering window, the minimum $I_{\min}$, the maximum value of $I_{\max}$ and the median value of I_{med} are determined. If the conditions are met

$$A_1 = I_{med} - I_{\min} \quad ; \quad A_2 = I_{med} - I_{\max} \; ; \; A_1 > 0 \quad \text{and} \quad A_2 < 0,$$

then the element of the central window I_{xy} is filtered, i.e. the value of the median is greater than the minimum and less than the maximum values in the window.

The ability of the median filter to suppress noise in images is expanded using hard and soft thresholds by determining the mean, Gaussians, medians, etc. These mechanisms preserve the sharpness of the boundaries of contrasting objects, replace the intensity value of the contour points with pixels in the vicinity of the median, and show the best performance in suppressing noise.

The possibility of the vector median filtering mechanism (VMF), which ensures the preservation of information about the contours of objects, and also uses the most important features when detecting objects, has also been investigated. Mathematically, such a filter is given by the equation

$$I_{new}(x,y) = med \underset{(kx,ky)\in K_{xy}}{\text{med}} \{I_{old}(kx,ky)\},$$

where I_{new} and I_{old}, – new and old values of the spectrum of pixels of the image; K_{xy} – kernel window with dimensions $K_{Hs} \times K_{Ws}$, centered at (x,y).

It was determined that the mechanism with VFM shows the best performance, preserves the clarity of the boundaries of contrasting objects, replaces the intensity values of points with pixels in the vicinity of the median.

To suppress additive noise, a Gaussian filtering mechanism is considered, which is given by the equation

$$I_{new}(x,y) = \sum_{dy=-RH}^{RH} \sum_{dx=-RW}^{RW} G(dx,dy) \cdot I_{old}(x+dx, y+dy),$$

where G – Gaussian function; RH and RW – constants that determine the rank of the filter vertically and horizontally.

When you want to specify the Gaussian equation in a two-dimensional dimension, then the product of two Gaussians in a one-dimensional dimension is performed.

Images can have low, high brightness and contrast. In this regard, it is recommended to use the mechanism for identifying images with a wavelet - the Retinex transformation in the HSV color space, which allows you to speed up the calculations. At the same time, in four image areas LL HL, LH and HH, alternating one-dimensional wavelet is formed -

transformation of rows and columns. To improve contrast, brightness distribution, equalization of histograms, Retinex filters with a mechanism for extracting linear and nonlinear features (edges, borders, contours of objects), as well as Sobel, Prewitt, Roberts, Canny with logical and shear transformations can be used [21, 22, 23-30].

A mechanism has been investigated and implemented that performs the following functions: aligns histology slices; finds contours of objects, a set of levels, thresholds, combines segmentation, conducts registrations, forms a search graph, performs approximations based on wavelet, shear and other transformations, determines parameters, performs color coding and color visualization of micro-objects.

At the same time, geometric, textural, morphological characteristics, edge maps in the image area are selected and used. Sets the nature of noise, dynamic range and many other details that negatively affect the results of image filtering.

The mechanism uses stretch ratio setting operators that are based on range limit, distribution center shift, zero alignment. At the output, the brightness of I_{MSR} is adjusted, which is set by pixels in a given range I_{TR} and the results of solving the equation are used [1, 3, 5, 9, 12, 13]

$$I_{MSR}(x,y,\sigma) = Cl\left(\frac{R_{MSR}(x,y,\sigma) - avg(R_{MSR}(\sigma))}{(\max(R_{MSR}(\sigma)) - \min(R_{MSR}(\sigma))) \cdot \Pr} \cdot I_{TR} + k_{offset} \right),$$

where k_{offset} – is the default luminance bias factor of $k_{offset} = 127$; $Cl()$ – function of cutting off values outside the desired range.

A set of 2D images presented to the filtering mechanism with a center "zero" and with a square deviation σ

$$G(x,y) = -\frac{1}{\pi \cdot \sigma^2}\left[1 - \frac{x^2 + y^2}{2\sigma^2}\right] e^{-\frac{x^2+y^2}{2\sigma^2}}.$$

The image identification mechanism with filtering performs the following functions: anti-aliasing; Search; suppression of "false" peaks; threshold filtering.

The possibility of the $\Psi_{a,s,t}$, $\Psi_{a,s,t} \in L_2(R^2)$ function of the mechanism is extended by the inclusion of operators of expansion, shift, transformation in the form

$$\Psi_{a,s,t}(x) = a^{-\frac{3}{4}}\Psi\left(A_a^{-1}S_s^{-1}(x-t)\right),$$

where $t \in R^2$ – broadcast; A_a – matrix of scaling or expansion; S_s - shift matrix, which are determined by the equation

$$A_a = \begin{pmatrix} a & 0 \\ 0 & \sqrt{a} \end{pmatrix}, \quad a \in R^+, \quad S_s = \begin{pmatrix} 1 & s \\ 0 & 1 \end{pmatrix}, \quad s \in R,$$

where $a \in R^+$ and $s \in R$.

The scale of A_a dilatation along two axes is controlled. In this case, the S_s shift matrix determines the orientation. The normalization factor $a^{-\frac{3}{4}}$ is set, which guarantees $\left\|\Psi_{a,s,t}\right\| = \left\|\Psi\right\|$

Let us present the results obtained in the development of constructive approaches, principles and methods for optimizing the identification of images of micro-objects using the mechanisms of discrete Fourier transform, segmentation and filtering.

2.2. Filtering mechanism based on discrete fourier transform

Let the $(u_{m,n})$ image be specified on the $0 \le m \le M-1, 0 \le n \le N-1$ plane, and the filtering mechanism with the function

$$SH(f)(j,k,m) = \left\langle f, \Psi_{j,k,m} \right\rangle.$$

This function for a fixed scale and all possible values of the shift and displacement parameters is given in the form

$$f_{cont} = \sum_{k=0}^{k_{\max}} \sum_{m=0}^{m_{\max}} SH_\Psi\left(f(j^*,k,m)\right)$$

where SH_Ψ – shift factor for the j^* scale; rotation (orientation) k and displacement m; $k_{\max}$ – maximum number of turns; $m_{\max}$ – maximum displacement value.

Discrete Fourier transform (DFT) for all $0 \le k \le M-1$ and $0 \le l \le N-1$ is given as [9, 10]

$$\hat{u}_{k,l} = \frac{1}{MN} \sum_{m=0}^{M-1} \sum_{n=0}^{N-1} u_{m,n} \exp\left(-\frac{2i\pi mk}{M}\right) \exp\left(-\frac{2i\pi nl}{N}\right).$$

And the inverse discrete Fourier transform (IDFT) $(u_{m,n})_{m,n}$ is given for all $0 \le k \le M-1$ and $0 \le l \le N-1$ in the form

$$u_{m,n} = \sum_{k=0}^{M-1} \sum_{l=0}^{N-1} \hat{u}_{k,l} \exp\left(\frac{2i\pi mk}{M}\right) \exp\left(\frac{2i\pi nl}{N}\right).$$

When noise interference is represented by a normalized two-dimensional Gaussian function with a deviation of σ, then it is given as, $G_\sigma(x,y) = \frac{1}{2\pi\sigma^2} \exp\left(-\frac{x^2+y^2}{2\sigma^2}\right)$, and its transformation in the form $\hat{G}_\sigma(\mu,\upsilon) = \exp\left(-\frac{\mu^2+\upsilon^2}{2\sigma^2}\right)$. The convolution of the image with the Gaussian $(u_{m,n})$, $0 \le m \le M-1, 0 \le n \le N-1$ and the interpretation of each $u_{m,n}$ on the $G = \{(m,n), 0 \le m \le M-1, 0 \le n \le N-1\}$ grid is given in the form of the following polynomial

$$u(x,y) = \sum_{k=0}^{M-1} \sum_{l=0}^{N-1} \hat{u}_{k,l} \exp\left(\frac{2i\pi mx}{M}\right) \exp\left(\frac{2i\pi ny}{N}\right).$$

Interpolating $(u_{m,n})_{m,n}$ on the grid G, u - representation of the limited band image. The convolution of a polynomial with a Gaussian kernel is given in the form

$$G_\sigma * u = \sum_{k=0}^{M-1} \sum_{l=0}^{N-1} \hat{u}_{k,l} G_\sigma * \exp\left(i\frac{2\pi k}{M}x + i\frac{2\pi l}{N}y\right) = \sum_{k=0}^{M-1} \sum_{l=0}^{N-1} \left(G_\sigma\left(\frac{2\pi k}{M}, \frac{2\pi l}{N}\right)\hat{u}_{k,l}\right) \exp\left(i\frac{2\pi k}{M}x + i\frac{2\pi l}{M}y\right),$$

where $G_\sigma\left(\frac{2\pi k}{M}, \frac{2\pi l}{N}\right)$ - DFT coefficients of convolution of the image, estimated at the frequency $\frac{2\pi k}{M}, \frac{2\pi l}{N}$.

The mechanism of filtering with a shift transform is investigated, based on the forward and inverse Fourier transforms, which expand as

$$\hat{\Psi}(\omega_1, \omega_2) = \hat{\Psi}_1(\omega_1)\hat{\Psi}_2\left(\frac{\omega_2}{\omega_1}\right),$$

where $\hat{\Psi}$ – Fourier transform; Ψ – one-dimensional wavelet; $\hat{\Psi}_1$ – any non-zero square-integrable function.

Discretization of the parameter t on a rectangular grid is performed as

$$j_0 = \left[\frac{1}{2}\log_2 \max\{M, N\}\right].$$

The spread and shift operators are specified by the following parameters:

$$a_j = 2^{-2j} = \frac{1}{4^j},\ j = 0,..., j_0 - 1,\quad s_{j,k} = k2^{-j},\ -2^j \le k \le 2^j,$$

$$t_m = \left(\frac{m_1}{M}, \frac{m_2}{N}\right),\ m \in G,\quad G = \{(m_1, m_2)\},\ m_1 = 0,..., M-1,\ m_2 = 0,..., N-1.$$

And the function itself in the form

$$\Psi_{j,k,m}(x) = \Psi_{a_j, s_{j,k}, t_m}(x) = \Psi\left(A^{-1}_{a_j, \frac{1}{2}} S^{-1}_{s_{j,k}}(x - t)\right).$$

2.3. Hybrid image segmentation and filtering engine

The points of the contour of the image are given by the distribution of the probability of the appearance of the $p(i) = \frac{x_i}{X}$, $x_i \ge 0$, $\sum_{i=1}^{L} x_i = 1$, x_i - i-th point of the contour; $X = [x_1, x_2, ..., x_i, ..., x_L]$ - the number of points of the contour.

When a sequence of contour points are set by pixels, then they are divided into parts of the C_0 - front and C_1 - background with a threshold for differentiating t, C_0 - pixel within $[1,2,...,t]$, C_1 – pixel within $[t+1,..., L]$, L - intensity of gray-level image dots within $[1,2,..., L]$, $p(i)$ is the probability of the appearance of gray-level dots x_i, $X = x_1 + x_2 + ... + x_L / L$ is the average number of points.

A mechanism for image identification with threshold contour segmentation and clustering based on C - average is proposed. The probability of occurrence of a point of a given class and average is given by the ratios:

$$w_0 = w(t) = \sum_{i=1}^{L} p(i);\qquad w_1 = 1 - w(t) = \sum_{i=t+1}^{L} p(i);$$

$$\mu_0 = \sum_{i=1}^{L} \frac{i\,p(i)}{w_0} = \frac{1}{w(t)};\qquad \mu_1 = \sum_{i=t+1}^{L} \frac{ip(i)}{w_1} = \frac{1}{1 - w(t)} \sum_{i=t+1}^{L} ip(i).$$

The overall average is given as $\mu_t = \sum_{i=1}^{L} i\, p(i)$, the probability of the overall mean is defined as $\mu_t = w_0\mu_0 + w_1\mu_1$, w_1, μ_1 – the probabilities of the foreground and background areas, probabilities μ_0, μ_1, μ_t - middle foreground, phono, the entire image level. The maximum threshold $t*$ is chosen in the form $t* = \arg\max \sigma_B^2$, $1 \le t \le L$. Between the classes C_0 and C_1, this value is specified as $\sigma_B^2 = w_0(\mu_0 - \mu_t)^2 + w_1(\mu_1 - \mu_t)^2$. Determined that the value median was found to be a reliable estimate compared to the mean level gray. For class C_k ($k = 0$ or 1).

In the considered mechanism, the median value is taken as the $t*$ threshold and the distribution C_k. The overall mean μ_t is replaced by the cumulative median m_t for all level gray. Similar to the average μ_t value of all image points.

The average values μ_0 and μ_1 are replaced by the median levels m_0 and m_1 of the front C_0 and back C_1 parts of the image, respectively. The value σ_B^2 of the two parts C_0 and C_1 is rewritten as $\sigma_B^2 = w_0(m_0 - m_T)^2 + w_1(m_1 - m_T)^2$, and the threshold $t*$ is selected based on the maximization condition

$$t* = \arg\max \sigma_B^2, 1 \le t \le L.$$

The results are also obtained on the identification mechanism with segmentation and filtering. For optimization, the edges of the image outline are determined. The original image is anti-aliased using the Canny filter. For each pixel of the points of the image contour, the magnitude and direction of the gradient are determined. Boundary pixels (extreme pixels) are selected, which are considered boundary pixels if the gradient value is greater than that of two adjacent pixels.

To improve the accuracy of image identification with segmentation and filtering, DWT is used and matrixes of interaction of points are compiled using the operator for extracting features and features of the input image. DWT coefficients are analyzed by calculating 13 statistical values.

The best classification accuracy of image identification is achieved with an offset operator of [2 0] and [2 0, 0 2].

The joint distribution of contour points at the operator of displacement (dx, dy) of an image (I) of size $N \times M$ is given in the form

$$C_{dx,dy}(i,j) = \sum_{p=1}^{N}\sum_{q=1}^{M}\begin{cases}1, & \text{if } I(p,q)=i \text{ and } I(p+dx,q+dy)=j,\\ 0, & \text{otherwise.}\end{cases}$$

It is proved that the matrix of connections of points of the contour is effective in statistical analysis.

It was determined that the implemented optimization mechanisms based on the discrete Fourier transform, median filtering with brightness correction by almost 10% reduces the image identification errors, mechanisms with hybrid segmentation, wavelet transforms, with color coding and brightness correction allow reducing the image identification errors to 8%.

The required efficiency of identification, recognition, classification of micro-objects is achieved through the use of mechanisms for the detection and use of statistical, dynamic, histological, specific characteristics of images.

2.4. Experimental research results

The experimental study is aimed at testing the implemented algorithms and software modules of the developed software complex for identification, recognition and classification of micro-objects, in particular, medical research of cellular elements of the inflammatory series (fibroblasts, fibrocytes) of lung disease. Scanning electron microscope Hitachi TH-3500 detects fragments of implants. The signs of chronic inflammation were assessed - the presence of giant cells. For this, more than 100 monochrome images are presented at various scales, which, depending on the analyzed details, have different resolutions.

The resolution value ranges from 500×700 to 5120×3840 pixels. When preparing samples of micro-objects, ultrathin sections and staining were performed.

The study consists in assessing tissue growth on the implant and determining the area of collagen fibers, the number of erythrocytes, etc.

Histological data were obtained that characterize tissue changes after implantation of an endo prosthesis based on titanium nickelide for 7, 14, 21 and 45 days.

Tables 1 show the values of characteristic parameters - brightness, such as mean value, standard deviation before and after correction, obtained using the Retinex filter.

Table 1. Brightness characteristics of histological images.

Images	Before correction		After correction	
	Average	Deviation	Average	Deviation
1	204.22	15.73	190.03	12.43
2	227.91	23.71	190.13	11.20
3	230.95	24.93	189.90	11.02
4	214.67	27.67	189.95	12.20
5, 6, 7	83.26	12.57	127.48	22.14
8 -14	112.89	21.17	127.02	29.53
15-21	63.25	24.71	126.95	37.20
22-45	70.10	14.30	127.54	25.42

The range of the average value of the brightness of the images was first reduced, which at the output of the mechanism is 0.24-0.46 units. A similar result is observed for images obtained with a scanning electron microscope.

A significant increase in the accuracy of image identification is achieved with a mechanism that uses shear transformation and color coding of images. Table 2 shows the results of these experimental studies, which were obtained using the Mathlab application package. The median filtering mechanism, taking into account the brightness correction by 12%, reduces identification errors based on the identification and use of image features. The mechanism with wavelet - transformation, color coding and brightness correction reduces image identification errors from 12% to 8%.

Table 2. Luminance characteristics of electron microscope images.

Periods (days)	Before correction		After correction	
	Average	Deviation	Average	Deviation
1	83.26	12.57	127.48	22.14
2	112.89	21.17	127.02	29.53
3	63.25	24.71	126.95	37.20
4	70.10	14.30	127.54	25.42
5, 6, 7	78.36-88.67	11.39-12.68	126.99-127.12	19.81-24.15
8-14	69.74-95.82	11.13-34.40	126.17-127.04	21.16-37.15
15-21	60.39-71.25	25.27-28.31	126.92-127.24	25.48-36.93
22-45	92.37-116.96	23.85-44.96	126.68-127.98	31.72-39.49

Table 3-4 shows the data of morphometric indicators of the identification error for the main investigated parameters. The quantitative characteristics of the contour, the total area of the implant, the contours and the proportion of tissue grown on the mesh were used. Estimates are obtained with a color-coded filtering engine and a brightness correction

Table 3. Estimation of the error of identification of morphometric parameters.

Periods (days)	Median filter mechanism		
	court	Callogenic fibers	Elastic fibers
7	8.0%	2.8%	10.3%
14	10.5%	2.2%	8.1%
21	13.4%	3.6%	14.4%
45	7.3%	1.2%	8.5%
Color-coded wavelet transform engine			
7	7.1%	2.5%	9.6%
14	9.6%	2.1%	7.6%
21	12.7%	3.4%	13.5%
45	7.1%	1.1%	7.9%
Mechanism with shift transformation, color coding, and brightness correction			
7	6.7%	2.3%	9.2%
14	9.2%	2.0%	7.3%
21	12.1%	3.2%	12.9%
45	6.8%	1.0%	7.5%

Table 4. Measurement of growth rate and morphometric parameters.

Periods (days)	Object area in pixels	Growing area in pixels	Not growing area in pixels	Growth rate	Not growth
Color-coded wavelet transform engine					
7	28277	19057	9220	67%	33%
14	40860	34364	6496	84%	16%
21	43322	38648	4674	89%	11%
45	51573	51397	176	98%	2%
Mechanism with shift transformation, color coding, and brightness correction					
7	29253	20125	9128	69%	31%
14	42875	36667	6208	86%	14%
21	44396	39946	4450	90%	10%
45	53585	53328	257	99%	1%

3. Conclusions

The scientific and methodological foundations for the identification of images, in particular of pollen grains, of unicellular medical objects, have been developed, which make it possible to build a fundamentally new computer technology for visualization, recognition and classification of micro-objects to significantly reduce the systematic error.

The technique is investigated and algorithms for traditional, Gaussian, median filtering are developed, and filters with wavelet, shear, Fourier transforms are implemented. It was determined that due to their use, the work of an expert-histologist, the processes of color coding

and correction of the brightness of the points of the image contour, are significantly simplified, and the use of time-consuming procedures of histological analysis is not required.

The developed software tools and algorithms are useful when processing large volumes of visual data, using brightness correction mechanisms based on filtering technology. It has been proved that the implemented software complexes for visualization, recognition and classification of images allow you to more clearly see the details of the objects under study in the images, evaluate tissue growth and express them with an average accuracy of 1-3%.

The developed software package increases the accuracy of image identification by two orders of magnitude, the speed of information processing by an average of 3-7%, the quality of noise filtering is achieved, as well as an increase in the contrast and brightness of the image. The use of the developed identification optimization mechanisms makes it possible to increase the accuracy of the choice of linear structures and the visual quality of the images of the micro-objects under study.

References

1. Barnard, K., Funt, B. Investigations into multi-scale retinex / K. Barnard, B. Funt // Colour Imaging: Vision and Technology. – 1999. – P. 9-17.
2. Vizilter, Yu.V. Image processing and analysis in machine vision tasks: A course of lectures and practical exercises / Yu.V. Vizilter. – Moscow: Fizmatkniga, 2010. – 672 p.
3. Bertalmio, M., Caselles, V., Provenzi, E. Int. Journal of Computer Vision. – 2009. – Vol. 83. – P. 101-119.
4. Shashev, D.V. Information-measuring equipment and technologies. Tomsk, 2016. – 544-550 p.
5. Kimmel, R., Elad, M., Shaked, D., Keshet, R., Sobel, I. Int. Journal of Computer Vision. – 2003. – № 52. – P. 7-23.
6. Jumanov, Isroil, Djumanov, Olim, Safarov, Rustam. 2nd Int. Conf on Energetics, Civil and Agricultural Engineering, E3S Web Conf. – 2021. – Vol. 304. https://doi.org/10.1051/e3sconf/202130401007
7. Popova, G.M., Stepanov, V.N. Automation and telemechanics. – 2004. – Vol. 1. – P. 131-142.

8. Kuleshov, S.V., Aksenov, Yu.A. Zaitseva, A.A. Innovative Science. – 2015. – Vol. 5. – P. 82-86.
9. Provenzi, E., Carli, L.D., Rizzi, A., Marini, D. Journal of the Optical Society of America. – 2005. – Vol. 22. – P. 2613-2621.
10. Bezuglov, D.A., Rytikov, S.Yu., Yukhnov, V.I., Shvidchenko, S.A. Modern problems of radio electronics: IV int. scientific conf., Rostov-on-Don. – 2012. – P. 203-212.
11. Jumanov, I.I., Djumanov, O.I., Safarov, R.A. Journal of Physics: Conference Series. – 2021. – Vol. 1791(1) 012099.
12. Verma, B., Blumenstein, M., Kulkarni, S.A. Journal of Intelligent Systems. – 1999. – Vol. 9(1). – P. 39-54.
13. Durai, A.S, Saro, A.E., Phil, M. GVIP Journal. – 2006. – Vol. 6(2). – P. 122-128.
14. Gonzalez, R. Digital image processing [Text] / P. Gonzalez, R. Woods. – M.: Tekhnosfera, 2005. – 1072 p.
15. Duda, R.O. Pattern Classification [Text] / R.O. Duda, P.E. Hart, D.G. Stork. – New York : John Wiley & Sons, 2001. – 654 p.
16. Liu D., Wang S., Huang D., Deng G., Zeng F., Chen H. Computers in Biology and Medicine. - 2016. - Vol.72. - pp. 185-200.
17. Ibragimovich, J.I., Isroilovich, D.O., Abdullayevich, S.R. Advanced in Intelligent System and Computing. – 2021. – 1323 AISC. – P. 170-179.
18. Banarse, D., France, I. Duller, A.W.G. Advances in engineering software. – 2000. – P. 944.
19. Boucher, A., Hidalgo, P., Thonnat, M., Belmonte, J., Galán, C. In 2nd European Symposium on Aerobiology. Vienna Austria. – 2000. – P. 3.
20. Kholmonov, S.M., Safarov, R.A. Science and World. – 2016. – Vol. I. – № 5(33). – P. 119-122.
21. Xu, Z., Bagci, U., Mansoor, A., Kramer-Marek, G., Luna, B., Kubler, A., Dey, B., Foster, B., Papadakis, G.Z., Camp, J.V., Jonsson, C.B., Bishai, W.R., Jain, S., Udu- pa, J.K., Mollura, D.J. Medical Physics. – 2015. – Vol. 42. – № 7. – P. 3896-3910.
22. Jumanov, I.I., Djumanov, O.I., Safarov, R.A. Chemical Technology, Control and Management. – 2019. – Vol 5. – P. 71-78.
23. Provenzi, E., Fierro, M., Rizzi, A., De Carli, L., Gadia, D., Marini, D. IEEE Transactions on Image Processing. – 2007. – Vol 16. – P. 162-171.

24. Marini, D., Rizzi, A. Image and Vision Computing. – 2000. – Vol. 18. – P. 1005-1014.
25. Ma, W., Morel, J.M., Osher, S., Chien, A. In Proceedings of IEEE Conference on Computer Vision and Pattern Recognition (CVPR, IEEE). – 2011. – P. 153-160.
26. Zhang, X., Shen, P., Luo, L., Zhang, L., Song, J. Proc. 21st Int. Conf. Pattern Recognit. (ICPR). – 2012. – P. 2034-2037.
27. Jumanov, I.I., Djumanov, O.I., Safarov, R.A. Int. Russian Automation Conf. – 2020. – P. 626-631.
28. Abdullah-Al-Wadud, M., Kabir, M.H., Dewan, M.A.A., Chae, O. IEEE Trans. Consum. Electron. – 2007. – Vol. 53. – № 2. – P. 593-600.
29. Li, L., Wang, R., Wang, W., Gao, W. Proc. IEEE Int. Conf. Image Process. – 2015. – P. 3730-3734.
30. Ibragimovich, J.I., Isroilovich, D.O. Abdullayevich, S.R. Int. Conf. on Information Science and Com. Tech. – 2020. – 9351483. – DOI:10.1109/ICISCT50599.2020.9351483